Research Article

Anandaraj Lakshmanan, Chandramohan Govindasamy, Allur Subramaniyan Sivakumar, Samer Hasan Hussein-Al-Ali, Monishsanthosh Ramesh, and Hariprasath Lakshmanan*

Anticancer and antimicrobial potential of zinc/sodium alginate/polyethylene glycol/ D-pinitol nanocomposites against osteosarcoma MG-63 cells

https://doi.org/10.1515/gps-2023-0124
received July 13, 2023; accepted September 4, 2023

Abstract

Background – The field of nanomedicine has attracted much interest and is now serving as the impetus for many revolutionary advances in the pharmaceutical industry.

Objectives – In the current exploration, we intended to fabricate the zinc/sodium alginate/polyethylene glycol/D-pinitol nanocomposites (ZSP/D-Pin/NCs) and evaluate their antimicrobial and anticancer properties against MG-63 cells.

Methods – ZSP/D-Pin/NCs were synthesized and characterized using several techniques and their cytotoxicity was examined against osteosarcoma MG-63 cells and normal 3T3 cells using the MTT assay. The levels of oxidative stress and apoptotic protein were examined using assay kits and fluorescence staining.

Results and Conclusion – The findings of several characterization studies revealed the development of agglomerated and crystalline ZSP/D-Pin/NCs. The antimicrobial assay demonstrated that ZSP/D-Pin/NCs substantially inhibited the growth of pathogens. Additionally, the MG-63 cell viability, which was exposed to several doses (1–20 µg) of ZSP/D-Pin/NCs, showed a remarkable decrease at various time periods, i.e., 24, 48, and 72 h without showing toxicity in 3T3 cells. The results of the fluorescence staining assay demonstrated that ZSP/D-Pin/NCs considerably increased apoptosis in the MG-63 cells by triggering oxidative stress. The antioxidants were reduced and upregulated the Bax and caspase expressions in ZSP/D-Pin/NC-treated MG-63 cells.

Keywords: nanomedicine, zinc nanoparticles, microbial infection, osteosarcoma, D-pinitol

1 Introduction

Nanotechnology is a popular study area in modern materials science [1]. Nanomaterials have recently been widely identified with distinctive characteristics and spectacular abilities, as they open the door for conducting transdisciplinary studies and resolving many practical issues [2,3]. The rapid increase of drug resistance in pathogens can be due to the overuse of antibiotics. Infections by bacteria are problems when it comes to therapy. The upsurge of antibiotic-resistant microbial infections has been one of the most significant public health complications in recent years [4–6]. The nanomedicine's exceptional qualities, such as their small size, high surface area, and strong mechanical stability, make them ideal for use in medicine for features like antibacterial activity [7].

Cancer is a serious illness worldwide, as it is the second-leading cause of mortality [8]. In children and young adults, osteosarcoma is a widespread and aggressive tumor of the bone. Patients' mobility is severely restricted by osteosarcoma, which frequently affects the distal femur, proximal tibia, and humerus [9]. Osteosarcoma has a high mortality rate and unfavorable prognosis, commonly due to metastasis to the lung and cancer recurrence. Patients

* **Corresponding author: Hariprasath Lakshmanan**, Division of Biochemistry, School of Life Sciences (Ooty off campus), JSS Academy of Higher Education and Research, Mysuru, India,
e-mail: hariprasath80@jssuni.edu.in
Anandaraj Lakshmanan, Monishsanthosh Ramesh: Division of Biochemistry, School of Life Sciences (Ooty off campus), JSS Academy of Higher Education and Research, Mysuru, India
Chandramohan Govindasamy: Department of Community Health Sciences, College of Applied Medical Sciences, King Saud University, P.O. Box 10219, Riyadh 11433, Saudi Arabia
Allur Subramaniyan Sivakumar: Department of Orthopaedic Surgery, Dongtan Sacred Heart Hospital, Hallym University, College of Medicine, Hwaseong, Republic of Korea
Samer Hasan Hussein-Al-Ali: Department of Chemistry, Faculty of Science, Isra University, Amman 11622, Jordan

with localized osteosarcoma tumors have a long-term survival rate at 5 years of about 60%, and lung metastasis at the time of diagnosis drastically lowers it to 20%. Additionally, during the past 30 years, the effectiveness of the treatment has remained constant due to chemotherapeutic drug resistance and low selectivity. Tumor recurrence and lung metastases are the primary causes of osteosarcoma therapy failure [10]. In order to combat osteosarcoma, innovative and effective treatments are urgently needed. Cancer treatment is made harder by the fact that conventional diagnostic procedures only discover cancers at advanced stages. Unlike other tumors, osteosarcoma has a complicated cytology that does not respond to traditional radiation and chemotherapy, and the adverse effects of several chemotherapeutic drugs are very dangerous [11,12].

Biomedical researchers are looking at ways to treat cancers despite several obstacles, such as poor oral bioavailability, insufficient water solubility, and non-specific biological transport and targeting [13]. Researchers have long been drawn to nanomedicine because of its practical uses for inexpensive drug delivery to specific organs, tissues, or cells for the treatment of cancer or for biocarriers that can traverse the blood–brain barrier. Nanoparticles (NPs) have a vast surface area and surface functionalization, which makes it easier to load drugs into them. Additionally, nanocomposites have recently developed rapidly for their exceptional properties and use in the medical field [14,15]. Zinc is one of the most important biometals in the human body [16]. Zinc and other biodegradable metals have lately received a lot of interest in tissue engineering [17]. Due to their distinctive optical and chemical characteristics, zinc NPs have received a lot of attention. Chemically, zinc has an abundance of −OH groups on its surface, which allows it to slowly dissolve in both acidic and strongly basic environments (such as those seen in tumor cells and their surrounding tissue) [18].

Alginate is a natural polysaccharide and is recognized as a potential biomaterial due to its superior biocompatibility, biodegradability, nontoxicity, and affordability in contrast to other materials [19]. In tissue engineering and regenerative medicine, alginates are frequently employed as cell scaffolding materials [20]. Polyethylene glycol (PEG) can be utilized to create a hydrated layer on the surface of NPs in order to decrease plasma clearance, enhance medication absorption, and avoid macrophage opsonization. PEG is also more beneficial in the NP drug delivery method due to its high biocompatibility and hydrophilicity [21]. D-Pinitol is an inositol that occurs naturally in a variety of plant species. It is particularly abundant in the pulp of the carob fruit (*Ceratonia siliqua*) that enables its separation and industrial production. D-Pinitol is well known to increase insulin sensitivity [22]. This natural inositol has been shown to have positive benefits on several disorders, including cancer, diabetes, osteoporosis, aging, hepatoprotection, and neurological diseases [23–27]. In the present exploration, we aimed to fabricate the zinc/sodium alginate/polyethylene glycol/D-pinitol nanocomposites (ZSP/D-Pin/NCs) and evaluate their antimicrobial and *in vitro* cytotoxicity activities against MG-63 cells.

2 Materials and methods

2.1 Chemicals

The following chemicals were bought from Sigma-Aldrich, USA: D-pinitol, zinc nitrate, sodium alginate, and PEG. The ELISA test kits used to measure the biochemical parameters were supplied by Thermofisher Scientific and MyBioSource, USA.

2.2 Synthesis of ZSP/D-Pin/NCs

For the synthesis of ZSP/D-Pin/NCs, first D-pinitol was dissolved in 20 ml of DMSO, which was then suspended in a 0.1% (wt/vol) solution of zinc nitrate. The mixture was continuously agitated until the development of the reaction suspension. The suspension was ultrasonically sonicated to reduce NPs, and the reaction solution containing zinc and D-pinitol was then added to the polymer solution, which was created using PEG and sodium alginate to coat the generated NPs. The coating process was performed using the microvolume flow titration technique. The final reaction mixture was dried using a spray pyrolysis method following the coating process in order to gather the powdered nanocomposite. The formulated ZSP/D-Pin/NCs were used for various characterization studies.

2.3 Characterization of fabricated ZSP/D-Pin/NCs

The UV-visible study was employed to verify that ZSP/D-Pin/NCs had developed in suspension. With the use of a UV-vis spectrophotometer (Shimadzu-1700, Japan), the ZSP/D-Pin/NCs were observed, and absorbance of the reaction solution at wavelengths between 200 and 1,000 nm was calculated.

A spectrofluorimeter (F-2500 FL Spectrophotometer, Hitachi) was used to measure the photoluminescence spectra of ZSP/D-Pin/NCs.

The elemental components of the formulated ZSP/D-Pin/NCs were determined by EDX, and the appearance and dispersion of ZSP/D-Pin/NCs were determined by SEM. A Carl Zeiss Ultra 55 FESEM device with EDX was used to determine the produced ZSP/D-Pin/NCs.

The distribution patterns and average size of the formed ZSP/D-Pin/NCs were examined using a Zeta Sizer (Malvern, USA) DLS. The formulated ZSP/D-Pin/NCs were investigated using an XRD (X'pert Pro PANalytical System) with a scan range of 2θ = 10–80° and Cu-Kα radiation of wavelength λ = 0.1541 nm.

2.4 Antimicrobial assay

By using the well-diffusion technique, the formulated antibacterial effects of ZSP/D-Pin/NCs were evaluated. About 1 ml of 5% DMSO solution was used to dissolve the ZSP/D-Pin/NC sample and utilized as a stock for bacterial strains such as *Staphylococcus aureus*, *Streptococcus pneumoniae*, *Klebsiella pneumoniae*, and *Streptococcus pneumoniae*, and SDA media was utilized for the fungal strain *Candida albicans*. After each strain was smeared over the culture medium, 6 mm wells were made on the surface of the media, and the wells were loaded with different doses (40, 50, and 60 µg) of formulated ZSP/D-Pin/NCs. The common antibiotic amoxicillin (30 µg/well) was utilized as a positive control. After the incubation period, the results were assessed, and the data were tabulated.

2.5 *In vitro* assays

2.5.1 Cell collection and maintenance

MG-63 cells and non-malignant fibroblast 3T3 cells were acquired from ATCC, USA. Then, cells were grown in DMEM enriched with FBS (10%) at 37°C in a CO_2 incubator. After the cells had reached 80% confluency, they were separated and used for the subsequent tests.

2.5.2 MTT assay

The viability of osteosarcoma MG-63 cells and normal 3T3 cells were exposed to ZSP/D-Pin/NCs and examined at three different time periods, i.e., 24, 48, and 72 h using the MTT assay. A 96-well plate containing MG-63 cells and 3T3 cells separately at a level of 5×10^3 cells were grown for 24 h before receiving different doses of the produced ZSP/D-Pin/NCs (1, 2.5, 5, 7.5, 10, and 20 µg) for additional 24, 48, and 72 h. After the treatment, DMEM (100 µl) and MTT reagent (20 µl) were applied to each well for 4 h. After liquefying the formed formazan stones in each well with 100 µl of DMSO, the absorbance at 570 nm was determined.

2.5.3 Analysis of mitochondrial membrane potential (MMP)

Rhodamine-123 (Rh-123) staining was used to examine the MMP levels in both control and ZSP/D-Pin/NC-treated MG-63 cells. The cells were loaded into a 24-well plate and treated with different doses (7.5 and 10 µg) of ZSP/D-Pin/NCs 24 h at 37°C. The cells were then stained for 30 min with Rh-123 at a concentration of 10 µg/ml. The MMP of both control and treated cells was examined using a fluorescence microscope.

2.5.4 Dual staining

The dual staining test was done in order to examine the apoptotic cell death in both control and treated cells. The MG-63 cells were loaded on DMEM medium in a 24-well plate and treated with 7.5 and 10 µg of ZSP/D-Pin/NCs for 24 h. Then, 100 µg/ml AO/EB (1:1) dye was added to each well to stain the cells for 5 min at 37°C. Finally, apoptotic cell death was confirmed by observing the cells under a fluorescence microscope.

2.5.5 DAPI staining

DAPI staining was performed to analyze the altered nuclear morphology and apoptosis in control and ZSP/D-Pin/NC-treated MG-63 cells. The cells were grown on a 24-well plate for 24 h and then exposed to 7.5 and 10 µg of ZSP/D-Pin/NCs for 24 h. After that, cells were fixed using paraformaldehyde (4%) for 30 min. After rinsing with saline, MG-63 cells were stained with DAPI (200 µg/ml) for 30 min. In the following step, a fluorescence microscope was utilized to observe chromatin condensation and remodeling in the treated cells.

2.6 Estimation of oxidative stress markers

The cell lysates were prepared using control and ZSP/D-Pin/NC-treated MG-63 cells by collecting and homogenizing the cells with saline solution. The levels of the lipid peroxidation marker TBARS and the antioxidants GSH and SOD in the control and ZSP/D-Pin/NC-exposed MG-63 cells were estimated

using the corresponding assay kits as per the protocols described by the manufacturer (Thermofisher, USA).

2.7 Estimation of apoptotic protein levels

The Bax, Bcl-2, caspase-3, and -9 expressions in the control and ZSP/D-Pin/NC-exposed MG-63 cells were determined using the corresponding assay kits as per the protocols recommended by the manufacturer (Thermofisher, USA).

2.8 Statistical analysis

After the values were evaluated with GraphPad Prism software, the results are shown as mean ± SD of three separate assays. With a significance level of $p < 0.05$, one-way ANOVA and DMRT were employed to analyze the changes in the values of the treatment groups.

3 Results

3.1 Characterization of formulated ZSP/D-Pin/NCs

3.1.1 UV-visible spectral analysis

The UV-visible spectra of ZSP/D-Pin/NCs are shown in Figure 1(a). At various wavelengths (200–1,000 nm), the absorbance of the synthesized ZSP/D-Pin/NCs was measured. The formation of ZSP/D-Pin/NCs was demonstrated by the maximum absorbance being observed at 369 nm (Figure 1a).

3.1.2 Photoluminescence (PL) analysis

The PL spectrum of synthesized ZSP/D-Pin/NCs is depicted in Figure 1(b). The presence of ZSP/D-Pin/NCs was demonstrated by excitations at 470, 504, 518, and 532 nm caused by ZSP/D-Pin/NCs. The crystal mode of the synthesized ZSP/D-Pin/NCs is revealed by the PL spectrum, together with structural and surface flaws. Exciton recombination may be seen in the peaks at 470 and 504 nm. Due to the interstitial oxygen vacancy, blue-green emissions were detected at 518 nm. In the synthesized ZSP/D-Pin/NCs, the peak at 532 nm shows the vacancy of singly ionized oxygen (Figure 1b).

3.1.3 SEM and EDX analysis

To examine the morphological appearance and elemental compositions of the developed ZSP/D-Pin/NCs, SEM and EDX tests were performed, and the results are shown in Figure 2. The formulated ZSP/D-Pin/NCs exhibited agglomerated morphology, which is evidenced by SEM images (Figure 2a). The occurrence of numerous elements, including carbon, nitrogen, oxygen, and zinc, was shown by the EDX analysis of ZSP/D-Pin/NCs (Figure 2b).

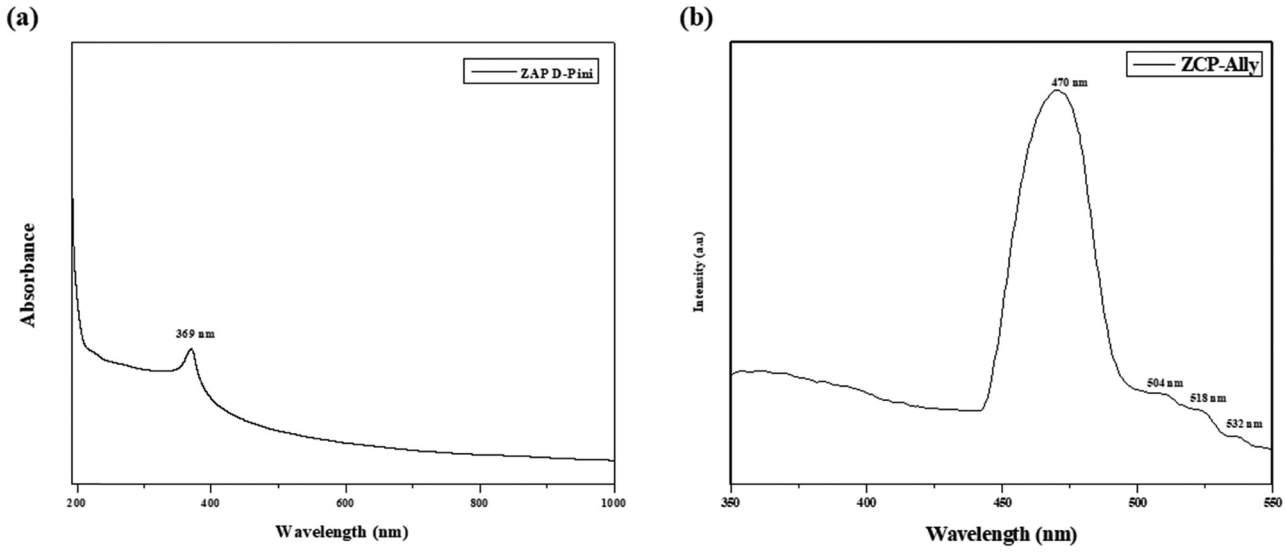

Figure 1: UV-visible spectrum and photoluminescence (PL) analysis of the synthesized ZSP/D-Pin/NCs. (a) UV-visible spectrum analysis of synthesized ZSP/D-Pin/NCs revealed the maximum absorbance peak at 369 nm. (b) The results of PL analysis of formulated ZSP/D-Pin/NCs showed several excitations at 470, 504, 578, and 532 nm, respectively.

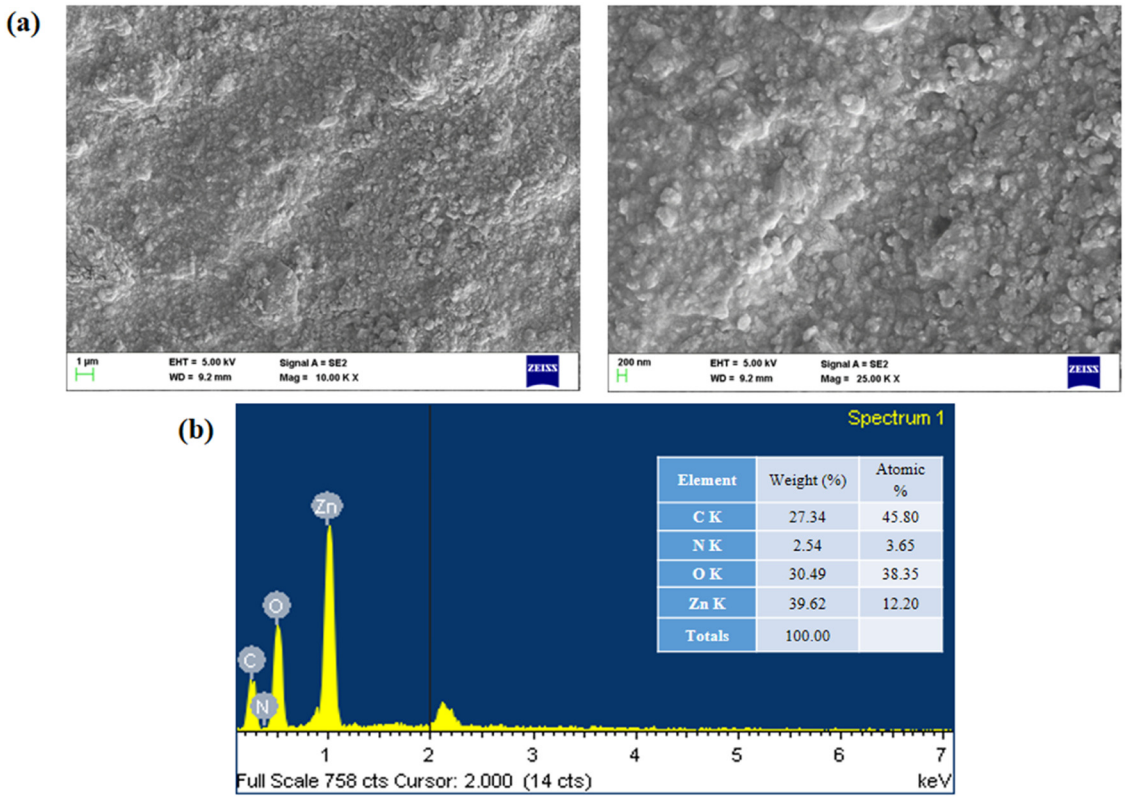

Figure 2: SEM and EDX analysis of the synthesized ZSP/D-Pin/NCs. (a) SEM images of the synthesized ZSP/D-Pin/NCs revealed the agglomerated morphological appearances. (b) EDX results showed the presence of carbon, nitrogen, oxygen, and zinc elements in the formulated ZSP/D-Pin/NCs.

3.1.4 XRD analysis

The XRD analysis results of the synthesized ZSP/D-Pin/NCs are shown in Figure 3, which support their purity and crystallinity. The characteristic peaks of the ZSP/D-Pin/NCs were observed at (100), (002), (101), (102), (110), (103), (200), (112), (201), and (202), demonstrating their crystalline nature.

3.1.5 DLS analysis

The DLS investigation results, which show the distribution of the fabricated ZSP/D-Pin/NCs, are shown in Figure 4. Discrete peaks with average sizes ranging from 100–160 nm that adhered to the narrower distribution were observed.

3.2 Antimicrobial activity of formulated ZSP/D-Pin/NCs

The antimicrobial properties of the formulated ZSP/D-Pin/NCs against pathogenic bacterial and fungal pathogens such as *S. aureus*, *Escherichia coli*, *K. pneumoniae*, *S. pneumoniae*, and *C. albicans* were investigated by the well diffusion method, and the results are shown in Table 1 and Figure 5. The findings demonstrated that the fabricated ZSP/D-Pin/NCs

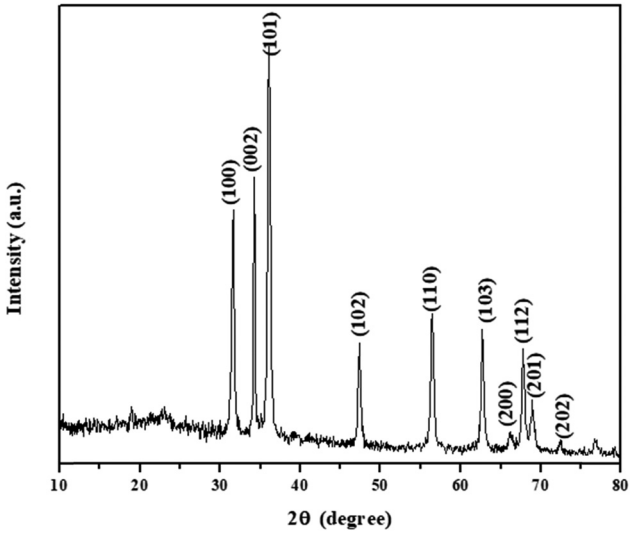

Figure 3: XRD analysis of the synthesized ZSP/D-Pin/NCs. The findings of XRD analysis revealed several peaks, which verify the crystalline nature of the synthesized ZSP/D-Pin/NCs.

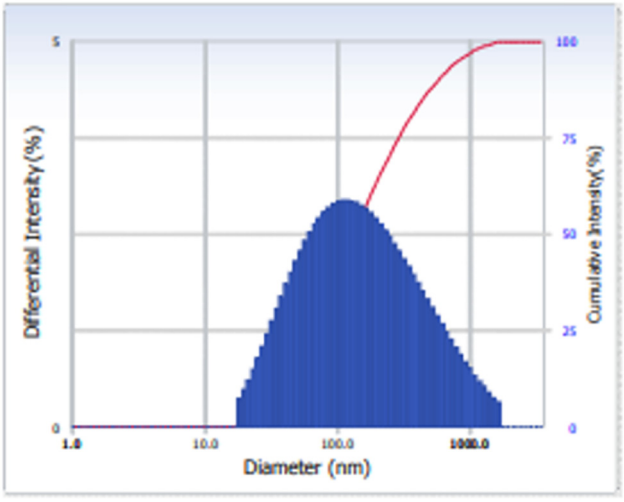

Figure 4: DLS analysis of the synthesized ZSP/D-Pin/NCs. The results of the DLS analysis demonstrated the distinctive peak that verifies the narrow distribution of the synthesized ZSP/D-Pin/NCs with sizes ranging from 100 to 160 nm.

have substantial antimicrobial properties, as they potentially inhibited the growth of the tested pathogens. On the growth plates, higher inhibitory zones were observed around increased doses of ZSP/D-Pin/NCs (40, 50, and 60 µg) loaded wells. The increased zone of inhibition was observed against *S. pneumoniae* (14 mm), *C. albicans* (14 mm), and *S. aureus* (13 mm), which were treated with the formulated ZSP/D-Pin/NCs (Figure 5).

Table 1: Antimicrobial activity of the synthesized ZSP/D-Pin/NCs

Pathogen	40 µg (mm)	50 µg (mm)	60 µg (mm)	A_{mx} (mm)
K. pneumoniae	8.5	9.5	9	16
S. pneumoniae	9	13	11	14
E. coli	9	9	9.5	13
S. aureus	13	13.5	14	14
C. albicans	11	13.5	14	9

The inhibitory zones (mm) of the tested pathogens are revealed, which were treated with 40, 50, and 60 µg of synthesized ZSP/D-Pin/NCs. The varied zone of inhibition was observed around the wells based on the pathogen characteristics and the concentration of ZSP/D-Pin/NCs.

Variable zones of inhibition are observed (Table 1) based on the nature of the strains and the concentration of ZSP/D-Pin/NCs.

3.3 Effect of ZSP/D-Pin/NCs on the viability of MG-63 cells

The viability of control and fabricated ZSP/D-Pin/NC-treated MG-63 cells and non-malignant 3T3 cells is shown in Figure 6. The treatment of 1, 2.5, 5, 7.5, 10, and 20 µg of prepared ZSP/D-Pin/NCs remarkably decreased MG–63 cell viability at various

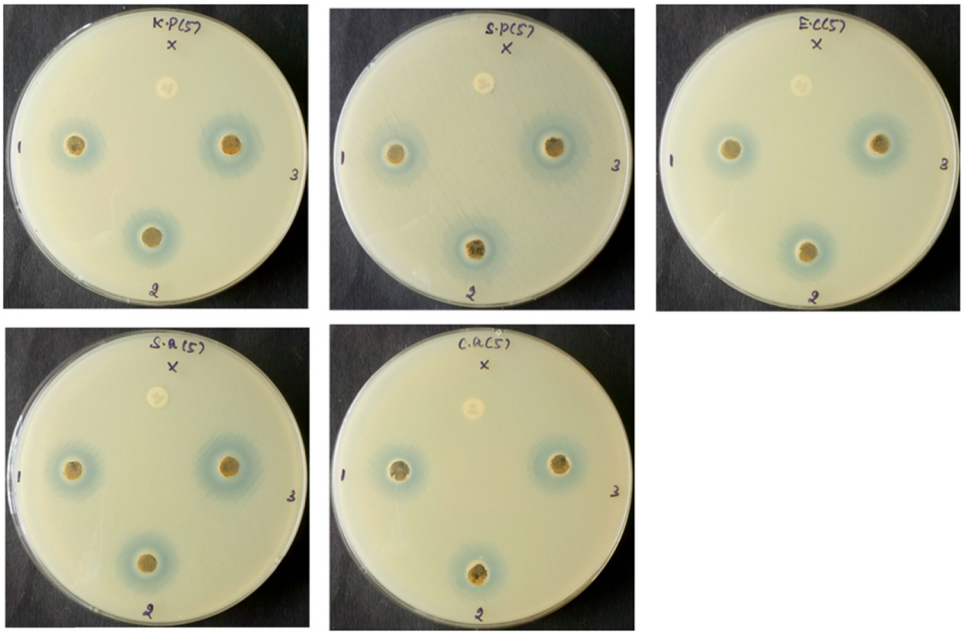

Figure 5: Antimicrobial activity of the synthesized ZSP/D-Pin/NCs. The antimicrobial properties of the synthesized ZSP/D-Pin/NCs were assessed against several pathogens such as *S. pneumoniae*, *K. pneumoniae*, *E. coli*, *S. aureus*, and *C. albicans*. The results indicate that ZSP/D-Pin/NCs substantially inhibited the growth of the tested pathogens.

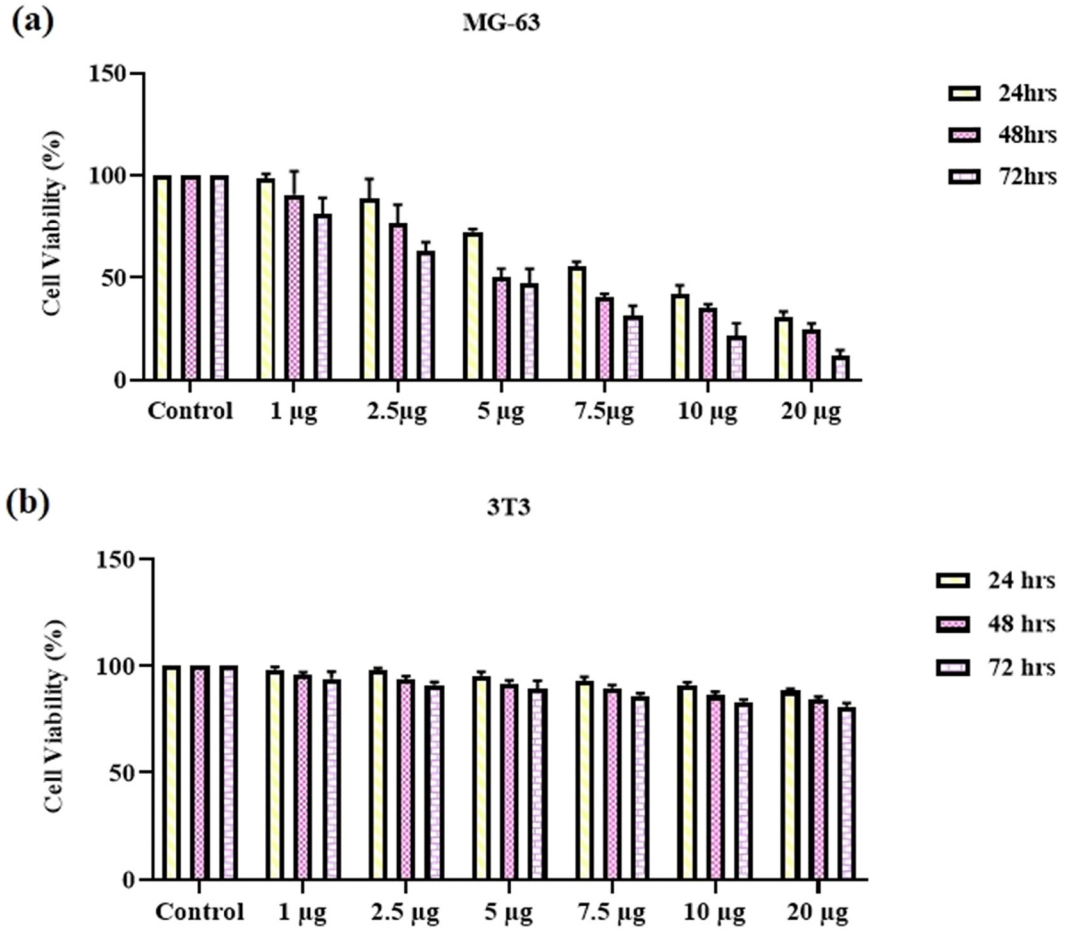

Figure 6: Effect of synthesized ZSP/D-Pin/NCs on the viability of MG-63 cells and normal 3T3 cells. (a) The MTT assay results revealed that the MG-63 cell viability was substantially decreased upon treatment with the synthesized ZSP/D-Pin/NCs at several doses, i.e., 5–30 µg at different time periods (24, 48, and 72 h). (b) The same dose of synthesized ZSP/D-Pin/NCs did not affect normal 3T3 cell viability; only a slight decrease in viability was observed after 48 and 72 h of treatment. Values are expressed as mean ± SD of triplicate measurements. Data are scrutinized statistically by one-way ANOVA and DMRT. *$p < 0.05$ when compared to the control.

time periods, i.e., 24, 48, and 72 h. The same doses of ZSP/D-Pin/NCs did not reduce the viability of 3T3 cells. When compared to 24 and 48 h of treatment, the 72 h treatment drastically reduced the MG-63 cell viability, and a mild reduction was noted in the viability of 3T3 cells over 48 and 72 h of treatment. The MG-63 cell growth was noticeably decreased by the higher dosages of the formulated ZSP/D-Pin/NCs, and the IC50 level of ZSP/D-Pin/NCs was found at 5–7.5 µg for 48–72 h (Figure 6).

3.4 Effect of ZSP/D-Pin/NCs on the MMP level in MG-63 cells

Figure 7 shows the changes in the MMP status in the control and ZSP/D-Pin/NC-exposed MG-63 cells. The exposure of MG-63 cells to 7.5 and 10 µg of ZSP/D-Pin/NCs resulted in significantly less green fluorescence and morphological changes compared to the control. These findings show that the MMP status in MG-63 cells treated with ZSP/D-Pin/NCs are reduced.

3.5 Effect of ZSP/D-Pin/NCs on the apoptosis in MG-63 cells

The results of AO/EB staining on apoptosis in control and treated MG-63 cells are shown in Figure 8. As shown in Figure 8, apoptotic cell death in MG-63 cells was significantly elevated after treatment with 7.5 and 10 µg of ZSP/D-Pin/NCs compared to control. The enhanced orange/yellow fluorescence, cell damage, and morphological changes in the ZSP/D-Pin/NC-treated cells reveal the increased number of cells with apoptosis.

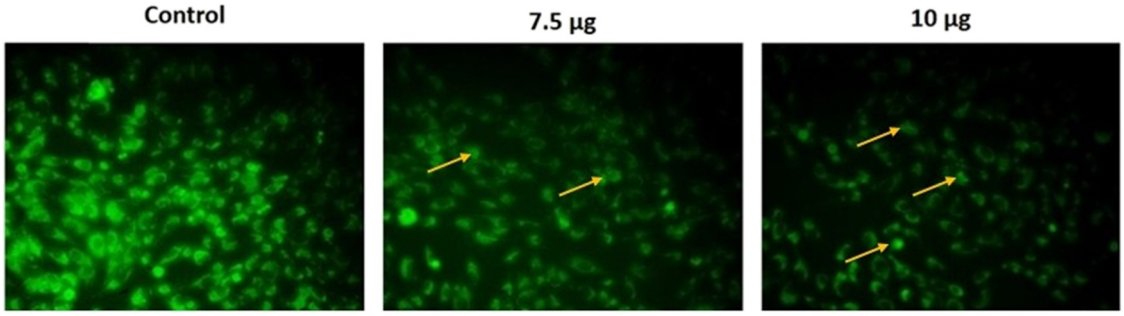

Figure 7: Effect of synthesized ZSP/D-Pin/NCs on the MMP level in MG-63 cells. Rh-123 staining was performed to analyze the changes in the MMP level in the control and treated cells. The ZSP/D-Pin/NCs-treated MG-63 cells showed decreased green fluorescence with morphological changes (yellow arrows) compared to the control, which proves the reduction in MMP levels.

3.6 Effect of ZSP/D-Pin/NCs on the apoptotic cell nuclear morphology of MG-63 cells

Figure 9 shows the results of ZSP/D-Pin/NC-induced apoptosis in MG-63 cells, which was detected by DAPI staining. When compared to the control, the MG-63 cells treated with 7.5 and 10 µg of ZSP/D-Pin/NCs showed an increased presence of apoptosis. The ZSP/D-Pin/NC treatment resulted in cell damage, alterations in the cell nucleus, and the development of apoptotic bodies, which verifies the occurrence of apoptosis.

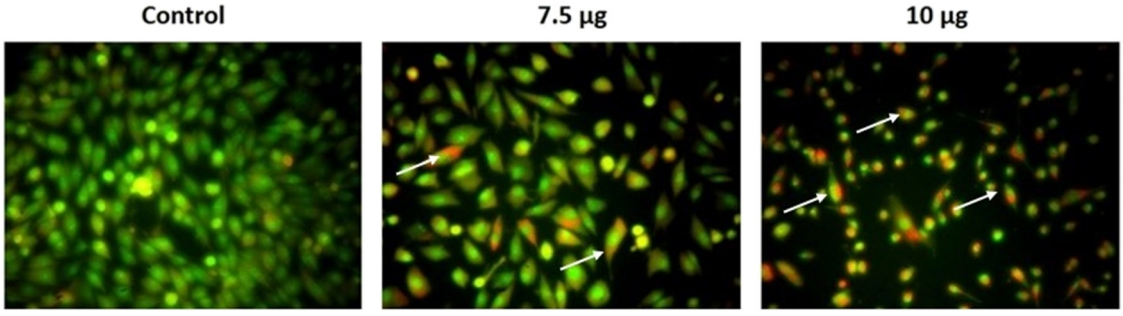

Figure 8: Effect of synthesized ZSP/D-Pin/NCs on the apoptosis in MG-63 cells. The dual staining assay was used to detect apoptosis in control and ZSP/D-Pin/NC-treated MG-63 cells. The images showed increased orange/red fluorescence in ZSP/D-Pin/NC-treated MG-63 cells (white arrows) compared to the control, which indicates the presence of an increased number of cells with apoptosis.

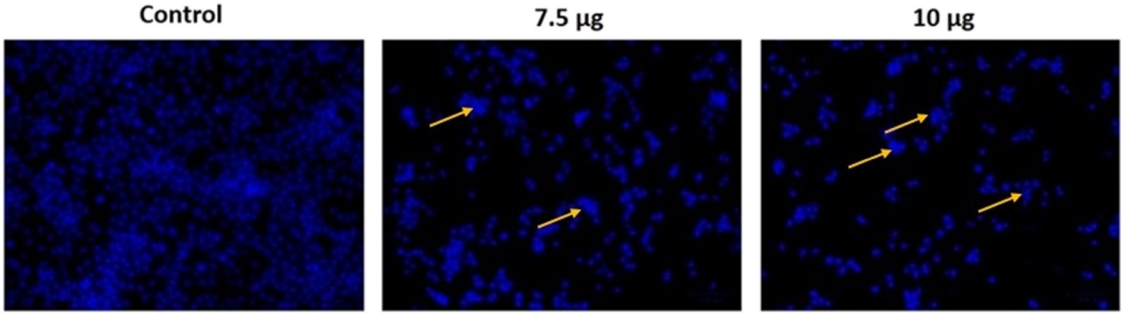

Figure 9: Effect of synthesized ZSP/D-Pin/NCs on the apoptotic cell nuclear changes in MG-63 cells. The changes in the apoptotic cell nuclear damages in the control and treated cells were assessed by DAPI staining. In comparison to the control, the ZSP/D-Pin/NC-treated MG-63 cells showed increased cell damage, altered nuclei, and the formation of apoptotic bodies (yellow arrows).

3.7 Effect of ZSP/D-Pin/NCs on the oxidative stress marker level in MG-63 cells

Figure 10 shows the results of an investigation on the changes in oxidative stress markers in the control and ZSP/D-Pin/NC-treated MG-63 cells. The MG-63 cells that were exposed to 7.5 and 10 µg of ZSP/D-Pin/NCs showed a substantial increase in the BARS level compared to the control. Furthermore, SOD and GSH levels in the MG-63 cells were considerably downregulated by the ZSP/D-Pin/NC treatment when compared to control. These results showed that ZSP/D-Pin/NCs facilitate oxidative stress-mediated cell death in MG-63 cells.

3.8 Effect of ZSP/D-Pin/NCs on apoptotic protein levels in MG-63 cells

The levels of apoptotic protein levels in the control and treated MG-63 cells were analyzed using corresponding assay kits, and the results are shown in Figure 11. In the 7.5 and 10 µg of ZSP/D-Pin/NC-treated MG-63 cells, apoptotic proteins such as Bax, caspase-3, and -9 were significantly higher than in the control, while Bcl-2 was lower. These results demonstrated that in MG-63 cells, ZSP/D-Pin/NCs increased the expression of apoptotic proteins and facilitated apoptosis.

4 Discussion

In this work, we formulated ZSP/D-Pin/NCs and characterized them using several techniques. UV-visible spectroscopy was used to investigate the optical characteristics. The produced ZSP/D-Pin/NCs displayed a single absorption band that was caused by the coherent oscillation of the ZSP/D-Pin/NCs' free electrons that were triggered by electromagnetic waves with energy in the visible spectrum [28]. The location of the wavelength at a maximum absorption (λ_{max}) in each bimetallic nanosystem relies on the

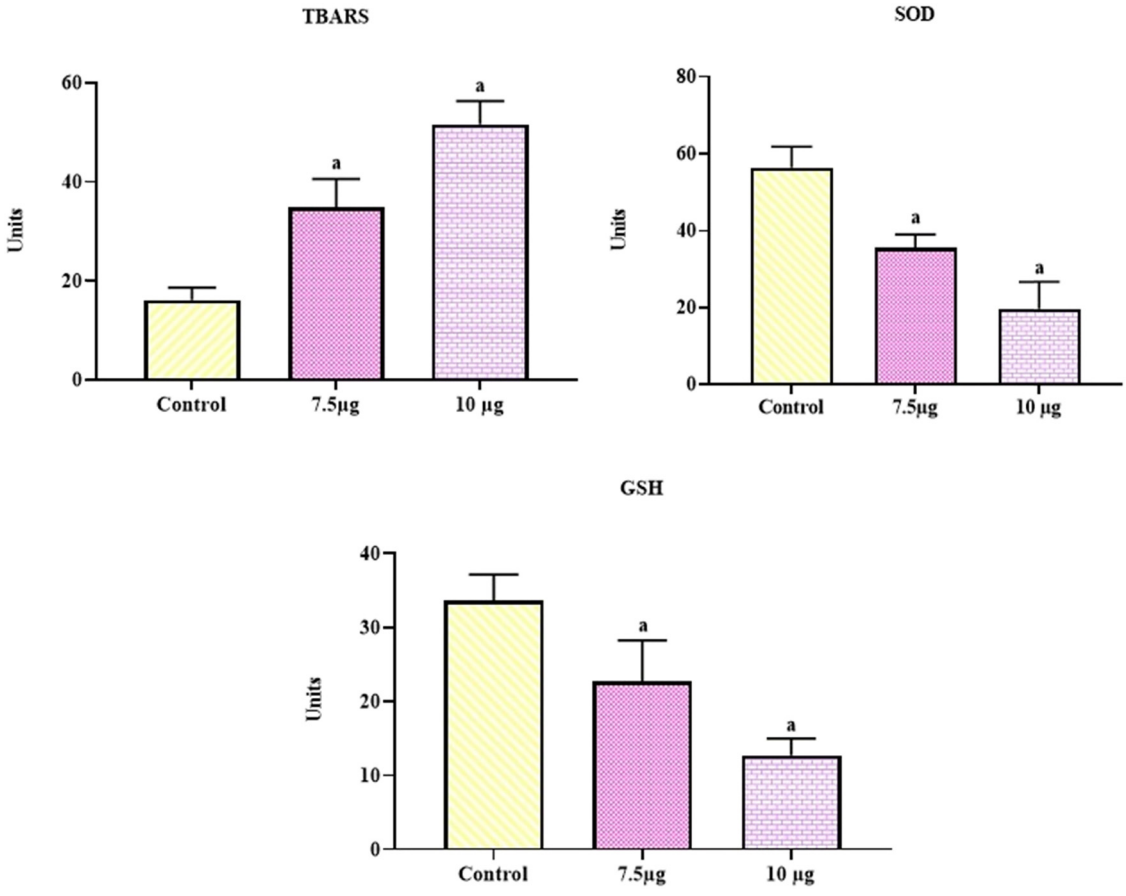

Figure 10: Effect of synthesized ZSP/D-Pin/NCs on the oxidative stress marker levels. Values are expressed as mean ± SD of triplicate measurements. Data are scrutinized statistically by one-way ANOVA and DMRT. * $p < 0.05$ compared with control.

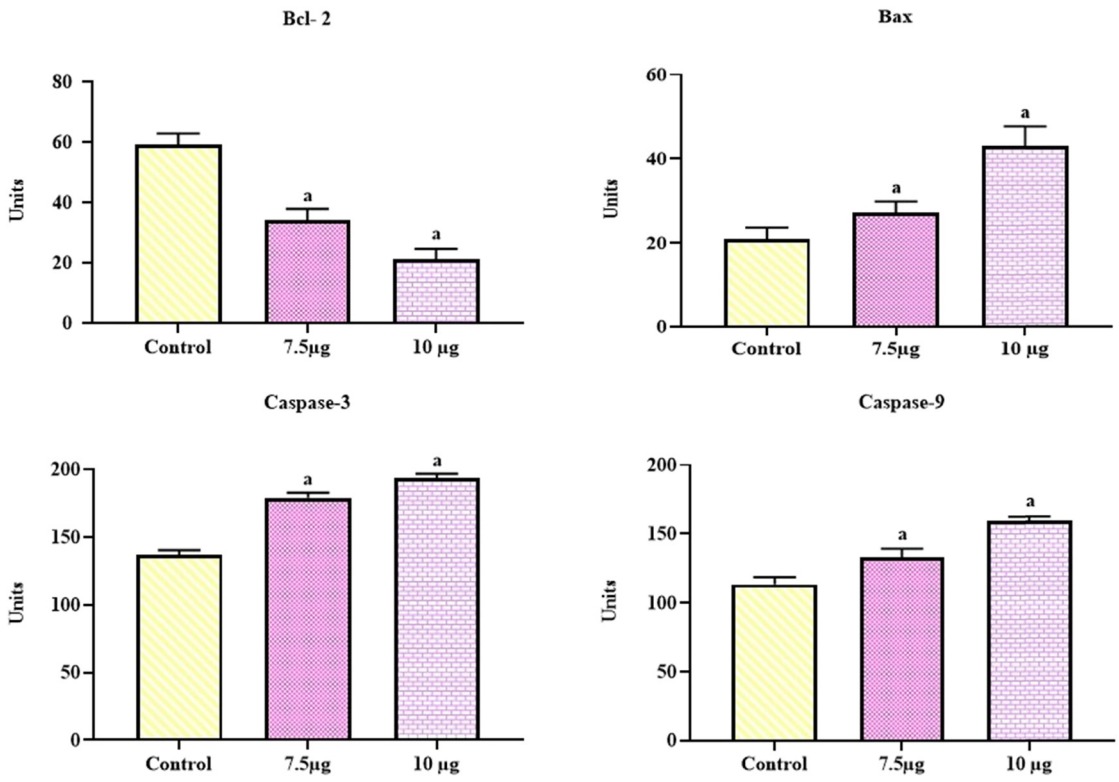

Figure 11: Effect of synthesized ZSP/D-Pin/NCs on the apoptotic protein levels. Values are expressed as mean ± SD of triplicate measurements. Data are scrutinized statistically by one-way ANOVA and DMRT. * $p < 0.05$ compared with control.

atomic makeup of the nanomaterials. Here, the maximum absorbance of the prepared ZSP/D-Pin/NCs was observed at 369 nm (Figure 1). ZSP/D-Pin/NCs were further characterized using XRD in order to investigate the samples' structure and phase composition (Figure 3). Figure 2 displays the resulting images from the FESEM analysis of the prepared ZSP/D-Pin/NCs' morphology and microstructure.

Currently, nanomedicines are employed extensively in several areas of medicine, and nearly all of them can be doped or decorated with substances that have potential medical applications [29]. It is also recommended to combine two or more components to enhance the therapeutic qualities of each material separately. NCs formed by conjugating NPs with antibacterial or anticancer moieties or natural compounds have been established as efficient materials for treating antibiotic resistance [30]. The field of nanomedicine has attracted a lot of interest and is now serving as an impetus for numerous evolutionary and revolutionary advances in the pharmaceutical industry. Because nanomedicine enhances the selective targeting of medication to cancer cells through the mechanisms of active internalization and passive permeation, it is utilized to treat cancer and bacterial infections. Additionally, nanomedicine improves cytotoxicity against cancer cells and reduces cell treatment resistance [31,32]. It is believed that the use of nanomaterials will revolutionize cancer treatment and diagnosis. In this sense, zinc NPs have proven to be one of the most promising choices in nanomedicine. The release of dissolved zinc ions and the stimulation of ROS, which causes the death of cancerous cells, are theorized to be the causes of zinc NPs' enhanced cytotoxicity to tumor cells [33].

WHO highlights that antimicrobial resistance is a foremost health issue worldwide [34]. It currently poses a danger to the efficiency of standard infection treatment and prevention around the world and has grown to be a global concern. However, in addition to being a challenging procedure, creating new antibiotics, biological products, or adjuvant medicines cannot keep up with the increasing rate of drug resistance. It is essential to find new alternatives since bacteria can become resistant to both natural and man-made antibiotics through a variety of methods, rendering them ineffective. Consequently, there is a huge demand for new, clinically approved antibiotic medicines. Recently, the delivery of antibacterial drugs has faced difficulties due to limited bioavailability and drug-related toxicities. Nano-formulations have emerged as a solution to these issues [35]. Here, our results demonstrated that ZSP/D-Pin/NCs effectively inhibited the

growth of the tested pathogens (Figure 5). Combinations of inorganic and organic NPs known as nanocomposites are already reported to have reliable antimicrobial activity [36,37]. The exact mechanisms of antibacterial activity of ZnO particles are not well understood yet, although some statements have been proposed, such as the production of hydrogen peroxide being the main factor of antibacterial activity [38] or the binding of ZnO particles on bacterial surfaces due to electrostatic forces being a mechanism [39].

Zinc is one of the micronutrients that the human body needs in order to function properly since it is necessary for the action of several enzymes, including alcohol dehydrogenase, carboxypeptidase, and carbonic anhydrase, which are crucial for eukaryotic metabolic processes [40]. Zinc-based nanocomposites have recently attracted interest in the biological and pharmaceutical sectors. Combining one material with another may improve its antibacterial, hydrophobic, tensile, and self-cleaning qualities. According to an earlier report, caprolactam–casein–ZnO–nanocomposite latexes have shown improved antibacterial activity, greater flexibility, and characteristics of hydrophobic casein films [41]. Similarly, we also discovered that the synthesized ZSP/D-Pin/NCs have strong antimicrobial properties against clinical pathogens (Table 1).

Osteosarcoma is the most prevalent primary bone cancer worldwide. The primary clinical therapeutic modalities are surgical resection and preoperative and postoperative adjuvant chemotherapy [42]. However, conventional chemotherapeutic agents have a number of adverse effects and inadequate targeting, which dramatically lower patient's quality of life. The development of targeted pharmaceuticals offers novel approaches to treat cancers. Nevertheless, some medications have poor absorption, low selectivity, and poor stability in tumor tissues [43]. Therefore, researchers have given special attention to novel therapies for cancer treatment. Recently, nanomedicines have demonstrated enormous potential in the detection, diagnosis, and cancer treatment [44]. Due to their great selectivity between tumor and healthy cells, the adverse effects are reduced, and the harm to healthy cells is avoided.

Nano-drug delivery systems for treating osteosarcoma are characterized by controllable drug release, biocompatibility, targeted changes in cancerous tissue, and better patient compliance. Insoluble drugs can be carried as nanomedicines to increase tissue permeability and passively target cancer locations [45]. The analysis of the cytotoxic profile of newly prepared sample drugs or nanomedicines is an essential step for successful drug development [46]. In this work, we analyzed the cytotoxicity of the formulated ZSP/D-Pin/NCs against both MG-63 and non-malignant 3T3 cells. The results showed a substantial diminution in the viability of osteosarcoma MG-63 cells but not affected the 3T3 cell growth (Figure 6). These findings revealed that ZSP/D-Pin/NCs inhibited the viability of osteosarcoma cells.

Oxidative stress is a major cause of cancer development. This phenomenon is characterized by excessive ROS production, altered cell metabolism and homeostasis, dysregulated gene expressions, and antioxidant instabilities [47]. Mild oxidative stress is constantly present in tumor cells, which appears to be beneficial to them and boosts their growth and metastasis, assisting tumor development [48]. In carcinogenesis, it is well established that alterations to antioxidant defense mechanisms facilitate tumor development. However, excessive oxidative stress is detrimental to cancer cells; the release of excessive ROS due to chemotherapy, irradiation, or the innate immune reaction is cytotoxic and results in cancer cell death [49].

The overproduction of ROS causes higher lipid peroxidation and TBARS formation, thereby damaging the cell structure and functions. The increase in TBARS is an indicator of excessive oxidative stress [50]. The primary defense of cells against oxidative stress is antioxidants, which maintain cellular homeostasis by removing excessive free radicals. GSH and SOD are well-known antioxidants that protect cells against oxidative damage [51]. Inducing high levels of ROS production to stimulate lipid peroxidation and apoptosis is a common strategy in current cancer treatment. Osteosarcoma cells are frequently resistant to oxidative damage caused by therapies [52]. In the current study, our outcomes proved that the ZSP/D-Pin/NC treatment increased the TBARS (51.91 ± 14) while decreasing the SOD (18.37 ± 2) and GSH (11.87 ± 3) in the MG-63 cells (Figure 10), thereby facilitating oxidative stress-mediated cell death.

Initiation and development of malignancies, including osteosarcoma, are profoundly influenced by apoptosis. Evasion of apoptosis is a common phenomenon in malignancies [53]. Accelerated tumor growth and metastasis are caused by the deregulation of apoptotic pathways. Apoptosis is an important mechanism for protecting tissues from abnormal proliferation by removing uncontrollably proliferating cells [54]. Apoptosis can be activated by several signaling pathways. Furthermore, mitochondria are crucial players in activating endogenous apoptotic pathways [55,56]. The major chemotherapeutic drugs usually work against cancer by activating apoptotic mechanisms in the tumor cells. In the current work, our results of DAPI and dual staining confirmed the onset of apoptosis in ZSP/D-Pin/NC-exposed MG-63 cells (Figures 8 and 9). Additionally, ZSP/D-Pin/NCs also diminished the MMP status in MG-63 cells (Figure 7). Hence, it was clear that ZSP/D-Pin/NCs could be used to treat osteosarcoma by promoting apoptosis.

It is well known that both intrinsic and extrinsic pathways play major roles in initiating apoptosis. There are key regulators in the Bcl-2 protein family that play main roles in mitochondria-mediated apoptosis. When cells undergo apoptosis, Bax is required for the permeabilization of the mitochondrial membrane [57]. It has already been reported that several anticancer drugs regulate the Bcl-2 family proteins to activate mitochondria-mediated apoptosis. Over the past decades, apoptosis induction has served a crucial role in osteosarcoma treatment, and its fundamental signaling axis has been extensively studied [58]. In the MG-63 cells, treatment with ZSP/D-Pin/NCs triggered Bax (41.61 ± 2) and caspase-3 (174.27 ± 15), and -9 (154.59 ± 12) expressions while inhibiting the expression of Bcl-2 (19.58 ± 4). Our findings revealed that apoptotic signaling in MG-63 cells was induced by the ZSP/D-Pin/NC treatment (Figure 11). Overall, ZSP/D-Pin/NCs were found to effectively inhibit viability and promote apoptosis in osteosarcoma MG-63 cells.

5 Conclusion

We synthesized ZSP/D-Pin/NCs and characterized them using several techniques. The findings of characterization studies revealed the formation of agglomerated and crystalline ZSP/D-Pin/NCs. The findings of antimicrobial activity revealed that the formulated ZSP/D-Pin/NCs efficiently inhibited the growth of various pathogens. Furthermore, ZSP/D-Pin/NCs substantially inhibited viability, decreased MMP levels, and promoted apoptosis in MG-63 cells. Overall, these findings revealed that SP/D-Pin/NCs have strong antimicrobial and anticancer properties. In addition, the lack of *in vivo* studies is one of the major limitations of this work, and further experiments still need to be performed in the future in order to develop ZSP/D-Pin/NCs as talented antimicrobial and anticancer agents.

Acknowledgement: The authors would like to thank the Head, School of Life Sciences (Ooty Campus) and the management of JSS AHER, Mysuru for providing the facilities and support.

Funding information: This project was supported by Researchers Supporting Project number (RSPD2023R712), King Saud University, Riyadh, Saudi Arabia.

Author contributions: Anandaraj Lakshmanan contributed in the conception, investigation, interpretation of data, supervision, work drafting, and submission; Hariprasath Lakshmanan contributed in the conception, design of the work, investigation, analysis, and work drafting; Monishsanthosh Ramesh contributed in design of the work, investigation and analysis, work drafting, and supervision; Chandramohan Govindasamy contributed in the formal analysis, interpretation of data, resources, and work drafting; Allur Subramaniyan Sivakumar contributed in interpretation of data, resources, administration, and work drafting; and Samer Hasan Hussein-Al-Ali contributed in interpretation of data, resources, and work drafting, conception, revising, and supervision. All authors read and approved the final manuscript.

Conflict of interest: The authors state no conflict of interest.

Data availability statement: The datasets generated during and/or analyzed during the current study are available from the corresponding author on reasonable request.

References

[1] Mukherjee S, Vinothkumar B, Prashanthi S, Bangal PR, Sreedhar B, Patra CR. Potential therapeutic and diagnostic applications of one-step in situ biosynthesized gold nanoconjugates (2-in-1 system) in cancer treatment. R Soc Chem Adv. 2013;3:2318.

[2] Ghotekar S, Pagar T, Pansambal S, Oza R. A review on green synthesis of sulfur nanoparticles via plant extract, characterization and its applications. Adv J Chem. 2020;2(3):128–43.

[3] Sahoo S. Socio-ethical issues and nanotechnology development: Perspectives from India. Conference on Nanotechnology. Institute of Electrical and Electronics Engineers; 2010. p. 1205–10.

[4] Burchacka E, Pstrowska K, Beran E, Faltynowicz H, Chojnacka K, Kulazynski M. Antibacterial agents adsorbed on active carbon: A new approach for *S. aureus* and *E. coli* pathogen elimination. Pathogen. 2021;10(8):1066.

[5] Jin SE, Jin HE. Antimicrobial activity of zinc oxide nano/microparticles and their combinations against pathogenic microorganisms for biomedical applications: From physicochemical characteristics to pharmacological aspects. Nanomaterial. 2021;11(2):1–35.

[6] Singh A, Gautam PK, Verma A, Singh V, Shivapriya PM, Shivalkar S, et al. Green synthesis of metallic nanoparticles as effective alternatives to treat antibiotics resistant bacterial infections: a review. Biotech Rep. 2020;25:e00427.

[7] Sharma R, Garg R, Kumari A. A review on biogenic synthesis, applications and toxicity aspects of zinc oxide nanoparticles. Exp Clin Sci J. 2020;19:1325.

[8] Singh P, Pandit S, Mokkapati V, Garg A, Ravikumar V, Mijakovi I. Gold nanoparticles in diagnostics and therapeutics for human cancer. Int J Mol Sci. 2018;19:1979.

[9] Letaief F, Khrouf S, Yahiaoui Y, Hamdi A, Gabsi A, Ayadi M, et al. Prognostic factors in high-grade localized osteosarcoma of the extremities: The Tunisian experience. J Orthop Sur. 2020;28:3.

[10] Lilienthal I, Herold N. Targeting molecular mechanisms underlying treatment efficacy and resistance in Osteosarcoma: A review of current and future strategies. Int J Mol Sci. 2020;21(18):6885.

[11] Yan J, Wang Y, Ran M, Mustafa RA, Luo H, Wang J, et al. Peritumoral microgel reservoir for long-term light-controlled triple-synergistic treatment of osteosarcoma with single ultra-low dose. Small. 2021;17(31):e2100479.
[12] Caliskan Y, Dalgic AD, Gerekci S, Gulec EA, Tezcaner A, Ozen C, et al. A new therapeutic combination for Osteosarcoma: Gemcitabine and Clofazimine co-loaded liposomal formulation. Int J Pharma Sci Res. 2019;557:97–104.
[13] Rahman HS, Othman HH, Hammadi NI, Yeap SK, Amin KM, Samad NA, et al. Novel drug delivery systems for loading of natural plant extracts and their biomedical applications. Int J Nanomed. 2020;15:2439–83.
[14] Krishnan P, Rajan M, Kumari S, Sakinah S, Priya SP, Amira F, et al. Efficiency of newly formulated camptothecin with β-cyclodextrin-EDTA-Fe_3O_4 nanoparticle-conjugated nanocarriers as an anti-colon cancer (HT29) drug. Sci Rep. 2017;7(1):10962.
[15] Nuthalapati S, Shirhatti V, Kedambaimoole V, Neella N, Nayak MM, Rajanna K, et al. Highly sensitive, scalable reduced graphene oxide with palladium nano-composite as strain sensor. Nanotech. 2020;31(3):035501.
[16] Tapiero H, Tew KD. Trace elements in human physiology and pathology: Zinc and metallothioneins. Biomed Pharma J. 2003;57:399–411.
[17] Saifullah B, Hussein MZ, Hussein-Al-Ali SH, Arulselvan P. Fakurazi. Antituberculosis nanodelivery system with controlled-release properties based on para-amino salicylate-zinc aluminum-layered double-hydroxide nanocomposites. Drug Des Dev Ther. 2003;7:1365–75.
[18] Kahsay MH, Tadesse A, Ramadevi D, Belachew N, Basavaiah K. Green synthesis of zinc oxide nanostructures and investigation of their photocatalytic and bactericidal applications. R Soc Chem Adv. 2019;9(63):36967–81.
[19] Tan JM, Karthivashan G, Arulselvan P, Fakurazi S, Hussein MZ. Characterization and *in vitro* studies of the anticancer effect of oxidized carbon nanotubes functionalized with betulinic acid. Drug Des Dev Ther. 2018;8:2333–43.
[20] Barahuie F, Hussein MZ, Hussein-Al-Ali SH, Arulselvan P, Fakurazi S, Zainal Z. Preparation and controlled-release studies of a protocatechuic acid-magnesium/aluminum-layered double hydroxide nanocomposites. Int J Nanomed. 2013;8:1975–87.
[21] Arcaute K, Mann BK, Wicker RB. Stereolithography of three-dimensional bioactive poly(ethylene Glycol) constructs with encapsulated cells. Ann Biomed Eng. 2006;34(9):1429–41.
[22] Navarro JA, Decara J, Medina-Vera D, Tovar R, Suarez J, Pavon J, et al. D-Pinitol from Ceratonia siliqua is an orally active natural inositol that reduces pancreas insulin secretion and increases circulating ghrelin levels in Wistar rats. Nutrient. 2020;12(7):2030.
[23] Jayasooriya RGPT, Kang CH, Park SR, Choi IH, Kim GY. Pinitol suppresses tumor necrosis factor-α-induced invasion of prostate cancer LNCaP cells by inhibiting nuclear factor-κB-mediated matrix metalloproteinase-9 expression. Trop J Pharma Res. 2015;14(8):1357–64.
[24] Choi MS, Lee MK, Jung UJ, Kim HJ, Do GM, Park YB, et al. Metabolic response of soy pinitol on lipid-lowering, antioxidant and hepatoprotective action in hamsters fed-high fat and high cholesterol diet. Mol Nutr Food Res. 2009;53(6):751–9.
[25] Liu SC, Chuang SM, Tang CH. D-Pinitol inhibits RANKL induced osteoclastogenesis. Int Immunopharmacol. 2012;12(3):494–500.
[26] Hada B, Yoo MR, Seong KM, Jin YM, Myeong HK, Min KJ. D-Chiro-inositol and pinitol extend the life span of Drosophila melanogaster. J Gerontol Ser Bio Sci Med Sci. 2013;68(3):226–34.
[27] Lopez-Gambero AJ, Sanjuan C, Serrano-Castro PJ, Suárez J, Rodríguez de Fonseca F. The biomedical uses of inositols: A nutraceutical approach to metabolic dysfunction in aging and neurodegenerative diseases. Biomed. 2020;8(9):295.
[28] Unser S, Bruzas I, He JL, Sagle L. Localized surface plasmon resonance biosensing: Current challenges and approaches. Sensors. 2015;15:15684.
[29] Carofiglio M, Barui S, Cauda V, Laurenti M. Doped zinc oxide nanoparticles: Synthesis, characterization and potential use in nanomedicine. App Sci. 2020;10:5194.
[30] Pozdnyakov A, Emel'yanov A, Ivanova A, Kuznetsova N, Semenova T, Bolgova Y, et al. Strong antimicrobial activity of highly stable nanocomposite containing AgNPs based on water-soluble Triazole-Sulfonate copolymer. Pharmaceutics. 2022;14:206.
[31] Anjum SM, Hashim SA, Malik M, Khan JM, Lorenzo BH, Abbasi C, et al. Recent advances in zinc oxide nanoparticles (ZnO NPs) for cancer diagnosis, target. Drug Delivery Treat Cancers. 2021;13:4570.
[32] Garbayo E, Pascual-Gil S, Rodríguez-Nogales C, Saludas L, Estella-Hermoso de Mendoza A, Blanco-Prieto MJ. Nanomedicine and drug delivery systems in cancer and regenerative medicine. Nanomed Nanobiotech. 2020;12:5.
[33] Mishra PK, Mishra H, Ekielski A, Talegaonkar S, Vaidya B. Zinc oxide nanoparticles: A promising nanomaterial for biomedical applications. Drug Discovery Today. 2017;22:1825–34.
[34] Piddock LJ. The crisis of no new antibiotics – What is the way forward. Lancet Infect Dis. 2012;12:249–53.
[35] Saifullah B, Hussein MZ, Hussein-Al-Ali SH, Arulselvan P, Fakurazi S. Sustained release formulation of an anti-tuberculosis drug based on para-amino salicylic acid-zinc layered hydroxide nanocomposites. Chem Cent J. 2013;7(1):72.
[36] Mei L, Lu Z, Zhang X, Li C, Jia Y. Polymer-Ag nanocomposites with enhanced antimicrobial activity against bacterial infection. ACS App Mat Interface. 2014;6:15813–21.
[37] Naskar A, Lee S, Lee Y, Kim S, Kim KS. A new nano-platform of erythromycin combined with Ag nano-particle ZnO nano-structure against methicillin-resistant Staphylococcus aureus. Pharmaceutics. 2020;12:841.
[38] Sirelkhatim A, Mahmud S, Seeni A, Kaus NHM, Ann LC, Bakhori SKM, et al. Review on zinc oxide nanoparticles: antibacterial activity and toxicity mechanism. Nano-Micro Lett. 2015;7:219–42.
[39] Stoimenov PK, Klinger RL, Marchin GL, Klabunde KJ. Metal oxide nanoparticles as bactericidal agents. Langmuir. 2002;18:6679–86.
[40] Maret W. Zinc biochemistry: From a single zinc enzyme to a key element of life. Adv Nutr. 2013;4:82–91.
[41] Wang Y, Ma J, Xu Q, Zhang J. Fabrication of antibacterial casein-based ZnO nanocomposite for flexible coatings. Mat Des. 2017;113:240–5.
[42] Wu X, Zhang X, Feng W, Feng H, Ding Z, Zhao Q, et al. A targeted erythrocyte membrane-encapsulated drug-delivery system with antiosteosarcoma and anti-osteolytic effects. ACS App Mat Interface. 2021;13(24):27920–33.
[43] Burns J, Wilding CP. Proteomic research in sarcomas – current status and future opportunities. Semin Cancer Bio. 2020;61:56–70.
[44] Ikram M, Javed B, Raja NI, Mashwani ZR. Biomedical potential of plant-based selenium nanoparticles: a comprehensive review on therapeutic and mechanistic aspects. Int J Nanomed. 2021;16:249–68.
[45] Lu ZR, Steinmetz NF, Zhu H. New directions for drug delivery in cancer therapy. Mol Pharma. 2018;15(9):3601–2.
[46] Yew YP, Shameli K, Miyake M, Khairudin NBBA, Mohamad SEB, Naiki T, et al. Green biosynthesis of superparamagnetic magnetite

Fe3O4 nanoparticles and biomedical applications in targeted anticancer drug delivery system: a review. Arab J Chem. 2020;13:2287–308.
[47] Mu XC, Isaac C, Schott T, Huard J, Weiss K. Rapamycin inhibits ALDH activity, resistance to oxidative stress, and metastatic potential in murine osteosarcoma cells. Sarcoma. 2013;2013:11.
[48] Hayes JD, Dinkova-Kostova AT, Tew KD. Oxidative stress in cancer. Cancer Cell. 2020;38:167–97.
[49] Jaganjac M, Borovic Sunjic S, Zarkovic N. Utilizing iron for targeted lipid peroxidation as anticancer option of integrative biomedicine: A short review of nanosystems containing iron. Antioxidant. 2020;9:191.
[50] Kuper H, Tzonou A, Kaklamani E, Hsie CC, Lagiou P, Adami HO. Tobacco smoking alcohol consumption and their interaction in the causation of hepetocellular carcinoma. Int J Cancer. 2000;85:498–502.
[51] Arulkumaran S, Ramprasath VR, Shanthi P, Sachdanandam P. Restorative effects of Kalpamiruthaa, and indigenous preparation, on oxidative damage in mammary gland mitochondrial fraction in experimental mammary carcinoma. Mol Cell Biochem. 2006;291:77–82.
[52] dos Santos Cavalcanti A, Meohas W, de Ribeiro GO, de Sá Lopes AC, Gholamin S, Razavi M, et al. Patient-derived osteosarcoma cells are resistant to methotrexate. PLoS ONE. 2017;12(9): e0184891.
[53] Bai Y, Liu X, Qi X, Liu X, Peng F, Li H, et al. PDIA6 modulates apoptosis and autophagy of non-small cell lung cancer cells via the MAP4K1/JNK signaling pathway. EBioMedicine. 2019;42:311–25.
[54] Celik B, Cicek K, Leal AF, Tomatsu S. Regulation of molecular targets in osteosarcoma treatment. Int J Mol Sci. 2022;23(20):12583.
[55] McArthur K, Kile B. Apoptotic caspases: multiple or mistaken identities. Trends Cell Biol. 2018;28(6):475–93.
[56] Strasser A, Vaux DL. Cell death in the origin and treatment of cancer. Mol Cell. 2020;78(6):1045–54.
[57] Jin PY, Lu HJ, Tang Y, Fan SH, Zhang ZF, Wang Y, et al. The effect of DNA-PKcs gene silencing on proliferation, migration, invasion and apoptosis, and *in vivo* tumorigenicity of human osteosarcoma MG-63 cells. Biomed Pharmacother. 2017;96:1324–34.
[58] White E, Lattime EC, Guo JY. Autophagy regulates stress responses, metabolism, and anticancer immunity. Trends Cancer. 2021;7(8):778–89.